# Temporal Summation of Subthreshold Stimuli in Human Motor Axons: Implications for Intraoperative Neuromonitoring

Naidoo A[1], Jones KE[2,3]

1. Department of Physiology, University of Alberta, Edmonton, Canada
2. Faculty of Kinesiology, Sport, & Recreation, University of Alberta, Edmonton, Canada
3. Neuroscience and Mental Health Institute, University of Alberta, Edmonton, Canada

Corresponding author:
Kelvin E Jones
University of Alberta
Faculty of Kinesiology, Sport, & Recreation
Van Vliet Center 4-220
116 St and 85 Ave
Edmonton, Alberta
T6G 2R3

Keywords: Intraoperative Neuromonitoring; Motor-evoked potential; Compound muscle action potential; Subthreshold stimulation; Superexcitability; Corticobulbar tract; Cranial nerve; Persistent sodium current

Number of tables: 2
Number of figures: 4
Words in abstract: 245

# Abstract

**Objectives**: To examine how stimulus amplitude and pulse width influence the properties of peripheral axons and the phenomenon of subthreshold superexcitability. The objective was to determine whether specific stimulus parameter combinations could minimize the likelihood of CMAP generation in response to subthreshold pulse trains, to inform safer settings for intraoperative corticobulbar MEP monitoring.

**Methods**: Fifteen healthy participants (convenience sample) received median nerve stimulation under nine conditions combining three amplitudes (80%, 85%, and 90% of threshold) and three pulse widths (0.1 ms, 0.5 ms, 1.0 ms). Trains of 1–7 subthreshold pulses (2 ms interstimulus interval) were delivered 10 times per condition. The number of CMAPs (>100 µV) per train length were recorded from the APB, and mean response probability was calculated as the primary outcome. A latent addition test estimated persistent sodium current contributions, via LAh to subthreshold superexcitability in each participant.

**Results**: Higher pulse amplitudes and wider pulse widths significantly increased CMAP probability, with a significant interaction between them ($F(4,56) = 4.853$, $p = .002$, partial $\eta^2 = .257$). All pairwise comparisons were significant ($p \leq .023$). When controlling for rheobase, LAh was positively correlated with response probability ($r_{partial}(12) = .539$, $p = .047$)

**Conclusions**: Subthreshold stimulus trains can directly activate motor axons, and this effect was quantified across pulse amplitudes and widths. A setting of 80% threshold and 0.1 ms pulse width yielded a low response probability (1.6%), suggesting it may reduce peripheral activation and improve the specificity of intraoperative corticobulbar MEP neuromonitoring.

**Abbreviations**

APB - Abductor pollicis brevis
CMAP - Compound muscle action potential
EMG - Electromyography
IONM - Intraoperative neuromonitoring
LAh - Latent addition induced change in threshold (with a 0.2 ms delay)
MEP - Motor-evoked potential
SSI - Subthreshold susceptibility index
TES - Transcranial electrical stimulation

# 1. Introduction/Background

Intraoperative neuromonitoring (IONM) of cranial nerves, particularly the facial nerve, is widely recognized as important for preserving neural function and reducing the risk of postoperative neurological deficits during brainstem and skull base surgeries (Chang et al., 1999; Isaacson et al., 2005; Neuloh et al., 2008). A standard approach is transcranial electrical stimulation (TES) delivered over lateral scalp positions to activate the precentral gyrus (Goto et al., 2010). However, TES can inadvertently excite peripheral portions of cranial motor nerves, leading to the generation of compound muscle action potentials (CMAPs) in target muscles even when the corticobulbar pathway is disrupted. This phenomenon risks misinterpretation of a CMAP as a true corticobulbar motor-evoked potential (MEP), potentially resulting in a false-negative assessment of neural integrity (Akagami et al., 2005; Dong et al., 2005).

The potential for peripheral activation during corticobulbar MEP monitoring was recognized early in the development of IONM protocols (Dong et al., 2005; Deletis et al., 2016). To distinguish central from peripheral responses, a verification step was introduced: if a train of stimuli elicits a muscle response but a single stimulus of the same intensity does not, the response is attributed to transsynaptic corticobulbar activation. This interpretation assumes that axonal excitability is fixed; specifically, that subthreshold stimuli have no cumulative effect on the axon. Under this assumption, if a single pulse fails to activate the axon, then a multipulse train at the same subthreshold intensity should also fail to evoke a response. However, this idea was challenged by work showing that repeated subthreshold stimulation can summate to directly activate motor axons (Téllez et al., 2016; Urriza et al., 2016; Urriza, 2020). In these studies, while a single subthreshold pulse never evoked a CMAP, trains of identical subthreshold pulses consistently did.

The physiological basis of this phenomenon, termed subthreshold superexcitability, was characterized by Bostock and colleagues in single human motor axons (Bostock et al., 2005). They showed that subthreshold electrical stimuli can transiently lower the threshold for action potential initiation. This effect includes a passive electrotonic component, proportional to the charge delivered by the stimulus, and an active component involving voltage-dependent sodium channels. One potential contributor to the active component is the persistent sodium current, a slowly inactivating conductance that activates near the resting membrane potential (Crill, 1996; Baker and Bostock, 1997; Goldin, 2003). When activated by subthreshold stimuli, these channels can produce a sustained depolarizing drive, further reducing the threshold and increasing the likelihood of axonal firing during subsequent stimulus pulses.

Building on the foundational work of Urriza et al., who showed that subthreshold trains (90% of threshold, 0.5 ms pulse width) could evoke CMAPs in the abductor pollicis brevis, we sought to

extend these findings by systematically varying both pulse amplitude and width. Unlike prior studies, which focused on representative EMG traces, we quantified response probability across trials and participants to assess the likelihood of CMAP generation from subthreshold stimulation. Our objectives were to determine how stimulus parameters affect axonal excitability, to quantify individual susceptibility to subthreshold superexcitability, and to explore whether this susceptibility correlates with persistent sodium currents. To that end, we included a latent addition (LAh) test to estimate the contribution of persistent sodium conductance to the observed excitability patterns.

# 2. Methods

## 2.1 Participants

Fifteen healthy participants (9 male and 6 female), aged 21-28 years, were recruited through convenience sampling. All participants provided written informed consent for experimentation, and their privacy rights were observed. Exclusion criteria were adopted from the MScan Multicenter protocol (Sørensen et al., 2023). Prior to testing, participants completed a pre-screening to assess use of medications associated with peripheral neuropathy and to rule out the following: history of central nervous system disease or injury, upper limb injuries resulting in numbness or weakness, previous chemotherapy, diagnosis of diabetes mellitus, self-reported alcohol intake exceeding 14 units per week, other causes of polyneuropathy, known nerve entrapment syndromes, cognitive impairment, or pregnancy. All procedures were performed in compliance with relevant laws and institutional guidance, and the study was approved by the Research Ethics Board of the University of Alberta (Protocol #: Pro00142797).

## 2.2 Surface Electrode Placements

Three types of electrodes were used: stimulation (3M Red Dot, 3M-2560), recording (Ambu® BlueSensor NF), and ground (Ambu® Neuroline Ground). Participants were positioned in a reclined examination chair with their feet elevated. The median nerve was mapped for stimulation proximal to the wrist to identify the optimal site for the stimulating cathode.

Skin preparation at both stimulation and recording sites included application of Nuprep skin gel, 70% isopropyl alcohol, and light abrasion using 3M Red Dot Trace Prep sandpaper tape to maintain impedance below 10 kΩ. Following preparation, non-polarizable silver/silver chloride electrodes were placed over the mapped stimulation site; the return (anode) was placed 10 cm proximally.

Surface EMG was recorded from the abductor pollicis brevis (APB) muscle. The active recording electrode (E1) was positioned over the mid-belly of the APB and optimized to yield the largest, fastest-rising CMAP. The reference electrode (E2) was placed over the metacarpophalangeal joint, and the ground (E0) was positioned on the dorsum of the hand.

To maintain consistent nerve temperature, the forearm was wrapped with Norm-O-Temp water-heating blankets set to 37 °C. Skin temperature was continuously monitored using a Digitimer D501 Isolated Temperature Monitor.

Stimulation was delivered via a Digitimer DS5 constant-current stimulator, controlled by QTracS software. Square-wave current pulses were applied to the median nerve. EMG signals were amplified (Digitimer D440-2; gain 300; bandpass 3–3000 Hz), filtered for 60 Hz line noise using a HumBug quasi-filter, digitized via a National Instruments USB-6251 BNC data acquisition board, and analyzed in real time using QTracS.

## 2.3 Urriza Protocol

The "Urriza" protocol was implemented using QTracW software. To conduct a 3x3 repeated-measures factorial experiment, each participant completed nine unique conditions, presented in randomized order. Conditions varied by pulse amplitude (80%, 85%, and 90% of threshold) and pulse width (0.1 ms, 0.5 ms, and 1.0 ms). Threshold was determined individually for each pulse width and defined as the current required to elicit a 100 μV CMAP in at least 80% of trials.

For each condition, stimulus intensity was set to 80%, 85%, or 90% of the pulse-width-specific threshold. Each block began with a single subthreshold pulse, followed by trains of 2 to 7 pulses with interstimulus intervals of 2 ms. Each stimulus train was repeated ten times, and the number of CMAP responses (≥ 100 uV) out of ten was recorded. This entire procedure was repeated three times per condition. Response probability for each train length was calculated as the average across the three repetitions. A single mean response probability for each participant was calculated as the average across all train lengths and conditions.

## 2.4 Latent Addition Protocol

Persistent sodium current was estimated using the latent addition protocol, as described by Bostock and Rothwell (1997). In brief, the protocol measures the interaction between two brief stimuli, a hyperpolarizing conditioning pulse followed by a test pulse, delivered at progressively increasing delays. Threshold changes are expressed as a percentage of a control threshold (defined as the current needed to elicit a target CMAP amplitude of 40% of maximum), and plotted on a semi-logarithmic scale as a function of inter-pulse interval. The resulting time course is fitted with a biexponential function representing a fast passive component ($\tau_1$) and a slower active component ($\tau_2$) that has been linked to persistent sodium conductance.

The primary outcome of interest was the threshold reduction at a 0.2 ms delay (LAh), a time point at which the passive component is nearly extinguished, allowing selective quantification of the active recovery component. LAh values were calculated for each participant to assess the magnitude of persistent inward current contributing to subthreshold excitability.

## 2.5 Statistical Analysis

Statistical analyses were performed using SPSS (version 29). A two-way repeated measures ANOVA was performed to evaluate the effects of pulse amplitude (80%, 85%, and 90% of threshold) and pulse width (0.1 ms, 0.5 ms, and 1.0 ms) on the mean probability of response to subthreshold stimulus trains. For each participant, condition-specific means were calculated by averaging response probabilities across train lengths (2-7 stimuli). Group means/medians were calculated across all 15 participants.

Assumptions for parametric statistical testing were evaluated prior to analysis. One outlier was identified among 135 data points (based on studentized residuals) but was retained as it did not affect the overall results. Shapiro-Wilk tests indicated one violation of normality ($p < .05$), but no data transformation was applied, given the robustness of repeated measures ANOVA to non-normality in within-subjects designs. Mauchly's test confirmed sphericity for the interaction term. Significant interactions were followed up using simple main effects analysis with pairwise comparisons adjusted using the Bonferroni correction.

To characterize the sensitivity of motor axons to subthreshold trains of stimuli, we defined a subthreshold susceptibility index (SSI) as the number of pulses in a train required to elicit a CMAP response with a 5% probability. This 5% criterion was chosen to reflect an acceptable threshold for false-negative responses during intraoperative neuromonitoring. For each stimulation condition, the group median response probability was plotted against the number of pulses in the train. These data were fit to a three-parameter asymmetric sigmoid function:

$$y = d + \left( \frac{a-d}{\left(1+\left(\frac{x}{c}\right)^{b}\right)^{m}} \right)$$

(Eq. 1),

where $y$ is the response probability, $x$ is the number of stimuli, and constants were set to $a = 0$, and $d = 100$, reflecting a response range from 0 - 100%. Parameters $b$, $c$, and $m$ were optimized by minimizing the sum of squared residuals using the GRG Nonlinear method (Vanderbei & Zhang, 1991). SSI was defined as the number of stimuli required to elicit a 5% response probability and was calculated by solving Eq. 1 for $x$ when $y = 5$:

$$x = c \times \left(1.05^{\frac{1}{m}} - 1\right)^{\frac{1}{b}}$$

(Eq. 2).

To examine whether persistent sodium currents contribute to inter-individual variability in subthreshold superexcitability, Pearson's correlation was used to assess the relationship between each participant's mean probability of response and their LAh value. Because rheobase is theoretically related to both variables, a partial correlation controlling for rheobase as a covariate was also performed. Linearity was assessed via scatter and partial regression plots; normality was evaluated using the Shapiro-Wilk test. Outliers were screened using boxplots (univariate) and Mahalanobis distance (multivariate).

All anonymized data and supplementary materials supporting the findings of this study are available in Figshare (Naidoo and Jones, 2025).

# 3. Results

## 3.1 Response Probability

Representative waveform data from a single participant illustrate the method used to quantify response probability after 10 repeated stimuli of each train length (Fig. 1). As the number of stimuli per train increased, the likelihood of evoking a CMAP in the APB muscle increased. Each condition (defined by a specific pulse width and amplitude) was tested three times to obtain a reliable estimate of the mean response probability for each participant. As summarized in Table 1, response probability increased systematically with both increasing pulse amplitude and longer pulse widths. Notably, only one condition (80% amplitude, with a 0.1 ms pulse width) had a group mean response probability below the 5% criterion used to define the Subthreshold Susceptibility Index (SSI).

[Figure 1 near here]
[Table 1 near here]

A two-way repeated measures ANOVA revealed a significant interaction between pulse amplitude and pulse width on response probability ($F(4,56) = 4.853$, $p = .002$, partial $\eta^2 = .257$). Follow-up analysis of simple main effects showed that pulse amplitude significantly influenced response probability at each pulse width (Fig. 2). At 80% of threshold, pulse width had a significant effect on the response probability, $F(2,28) = 29.399$, $p < .001$, with all pairwise comparisons reaching significance ($p \leq .015$). At 85% and 90% of threshold, the effects of pulse width were also significant, $F(2, 28) = 43.881$, $p < .001$ and $F(2, 28) = 34.243$, $p < .001$, with all pairwise comparisons statistically significant ($p \leq .002$ & $p \leq .023$, respectively). Overall, the pattern of results indicates that both greater amplitude and longer pulse width increase the likelihood of evoking a CMAP, with all pairwise comparisons across conditions showing statistical significance ($p \leq .023$; Fig. 2).

[Figure 2 near here]

The results above report mean response probability, which is averaged across the number of stimuli in each train and therefore does not reveal how response probability evolves with increasing stimulus number. To address this, we examined how the number of stimuli per train affects the likelihood of evoking a CMAP for each combination of pulse amplitude and pulse width. The median response probability for each condition was plotted as a function of stimulus number and fit with a sigmoid function (Equation 1). Figure 3 shows these response curves, separated by pulse width (Panels A–C) and colour-coded by pulse amplitude. At each pulse width, higher amplitudes yielded steeper curves, indicating that fewer stimuli were needed to reach high response probabilities.

[Figure 3 near here]

To summarize these effects, we computed the Subthreshold Susceptibility Index (SSI), defined as the number of stimuli required to reach a 5% probability of eliciting a CMAP. This threshold is indicated by the intersection of each fitted curve with the horizontal dotted grey line (Fig. 3), and the resulting SSI values are reported in Table 2. Lower SSI values indicate *greater* susceptibility to subthreshold stimulation, i.e. fewer stimuli are needed to reach the 5% response probability criterion. SSI values decreased systematically with increasing pulse amplitude and pulse width, reflecting the additive effects of these parameters on temporal summation. For example, at the highest-intensity condition (90% threshold, 1.0 ms pulse width), fewer than 2 stimuli were required to reach the 5% threshold. In contrast, at lower intensities (e.g. 80% and 0.5 ms), about 5 stimuli were required. For the lowest-intensity condition (80% and 0.1 ms), CMAP responses were too infrequent to permit a stable curve fit, and no SSI value could be estimated.

[Table 2 near here]

## 3.2 Latent Addition Results

A Pearson correlation indicated a moderate, positive association between mean response probability and LAh ($r(13) = .475$, $p = .073$). Controlling for the fast time constant ($\tau_1$) slightly reduced the strength of the correlation ($r_{partial} = 0.404$). This suggested that $\tau_1$ was not a major contributor to subthreshold superexcitability. After controlling for rheobase, the partial correlation strengthened and reached statistical significance ($r_{partial}(12) = .539$, $p = .047$) (Fig. 4). LAh accounted for approximately 22.5% of the variance in response probability in the bivariate analysis, and 29.0% after adjusting for rheobase.

[Figure 4 near here]

# 4. Discussion

This study demonstrated that the likelihood of evoking a compound muscle action potential (CMAP) in response to trains of subthreshold stimuli increases with both greater stimulus amplitude and longer pulse width, and that these two parameters interact in a nonlinear manner to modulate excitability. Importantly, individuals with greater susceptibility to this form of temporal summation, reflected by higher response probabilities and lower Subthreshold Susceptibility Index (SSI) values, also exhibited larger persistent sodium currents, as estimated by the LAh metric. This represents the first empirical association between the subthreshold superexcitability phenomenon and an established biophysical marker of persistent inward sodium conductance, providing a partial mechanistic explanation for inter-individual variability in susceptibility to peripheral nerve activation by subthreshold stimulus trains.

## 4.1. Subthreshold Superexcitability

These findings extend the foundational work by Urriza et al. (2016), who first described CMAP generation from trains of subthreshold stimuli using a single stimulation condition (90% of threshold amplitude, 0.5 ms pulse width). That study demonstrated the potential for peripheral nerve activation without transsynaptic activation of corticobulbar pathways, raising concerns for intraoperative neuromonitoring (IONM). Our factorial design addressed unanswered questions by systematically varying amplitude and pulse width to determine how these parameters interact to influence response probability, quantified using mean response probability and the SSI.

We, somewhat arbitrarily, defined a clinically meaningful activation risk as a 5% response probability and calculated SSI values to determine how many stimuli for each condition could be safely used before reaching this threshold. Without any limit on train length, only the lowest stimulation condition tested (80% amplitude, 0.1 ms) met this safety threshold for trains up to seven stimuli; in this case, SSI could not be estimated because responses never reached 5%. All other conditions crossed the 5% threshold with fewer than seven pulses, showing that modest changes in stimulus parameters can substantially alter subthreshold superexcitability.

From a practical standpoint, IONM practitioners may prefer to limit train length rather than rely on a single '*safe*' amplitude/width setting. Table 2 provides a framework: if the upper limit is set to four pulses per train, as originally suggested by Dong et al. (2005), any condition with an SSI $\geq 4.0$ can be considered acceptable. Under this criterion, three combinations may be used: 80% with 0.1 ms, 80% with 0.5 ms, and 85% with 0.1 ms, giving greater flexibility. With a limit of three pulses, an even broader set of combinations qualifies, allowing for individualized trade-offs between risk and successful monitoring.

These findings also highlight inconsistencies in current practice. Protocols for corticobulbar tract monitoring vary widely — 3–5 pulses, pulse widths from 0.05 to 0.5 ms, and interstimulus

intervals of 1–2 ms — yet rarely specify amplitude as a percentage of single-pulse motor threshold (Izzo et al., 2024; Verst et al., 2012; Dong et al., 2005). This omission is notable, given that amplitude is a key determinant of susceptibility and was central to the original warning that threshold in peripheral nerves is not fixed and that subthreshold superexcitability needs to be considered when interpreting IONM responses (Téllez et al., 2016). The lack of standardized, threshold-referenced amplitude reporting hampers reproducibility and may contribute to variability in false-negative rates across centers.

## 4.2. Persistent Sodium Currents

While the results above provide IONM practitioners with practical options for minimizing risk, they do not explain why some individuals remain more susceptible to subthreshold activation than others. Inter-individual variability was anticipated from the outset, but its mechanistic basis has remained largely speculative in the literature (Téllez et al., 2016; Urriza et al., 2016; Urriza, 2020). To address this gap, we added an empirical measure, the LAh metric from latent addition testing (Bostock and Rothwell, 1997), as a potential physiological marker of susceptibility.

The significant, though moderate, correlation between LAh and the mean response probability suggests that persistent sodium currents in the axon provide a partial mechanistic explanation for subthreshold superexcitability. These currents reflect a sustained inward sodium conductance that does not inactivate rapidly, allowing subthreshold stimuli to summate over successive pulses (Crill, 1996; Baker and Bostock, 1997; Goldin, 2003). We had anticipated a stronger association; in this sample, LAh accounted for 22.5% of the variance in mean response probability, increasing to 29% after adjusting for rheobase (Fig. 4). Although these values fall short of a complete explanation, they advance the field by providing an empirical link between this phenomenon and an intrinsic biophysical property of motor axons. The remaining unexplained variance points to other contributing factors, such as potassium conductances, nodal architecture, or differences in internodal capacitance, that merit investigation in future studies.

# 5. Conclusion

This study quantified the parameter dependence of subthreshold superexcitability and identified persistent sodium conductance as a partial mechanistic contributor. By showing that CMAP probability increases with higher amplitude and longer pulse width, and by defining SSI-based criteria for '*safe*' train lengths, we provide IONM practitioners with practical strategies to reduce false-negative responses. At the same time, our results challenge the persistent assumption that a single-pulse threshold defines a fixed level of excitability, underscoring the need for threshold-referenced, standardized stimulation protocols. The mechanistic link to LAh extends previous literature but also highlights that susceptibility is multifactorial, warranting further investigation to improve patient outcomes.

# Glossary

**Compound muscle action potential (CMAP) -** The response measured from a muscle following stimulation of its innervating motor neuron axon
**Latent Addition -** A test that estimates persistent sodium current magnitude
**Motor evoked potential (MEP) -** The response measured from a muscle following a synapse between upper and lower motor neurons
**Rheobase -** The minimum electrical current required to stimulate a nerve or muscle cell to fire an action potential
**Subthreshold stimulation -** Stimulation at an intensity below the threshold required to elicit an action potential
**Subthreshold superexcitability -** A period of axonal excitability marked by a reduction in threshold
**Subthreshold superexcitability index (SSI) -** The number of stimuli in a train required to elicit a 5% probability of a CMAP

# Data availability statement

Anonymized data and supporting documents for this study are openly available in Figshare at https://doi.org/10.6084/m9.figshare.29897132.

# Declaration of generative AI and AI-assisted technologies in the writing process

During the preparation of this manuscript, the authors used ChatGPT (OpenAI, San Francisco, CA, USA) to assist with improving clarity, organization, and grammar in selected sections. All AI-generated suggestions were reviewed, edited, and approved by the authors, who take full responsibility for the content of the final manuscript.

# Acknowledgements

We would like to thank Dr. Siyu Du, whose work as a clinical research coordinator facilitated various aspects of the study. We would also like to extend our gratitude to Dr. James Howells, who facilitated the improvement of QTracS, allowing us to obtain images for this paper. Lastly, we would like to express our appreciation to all the participants who took part in this study.

# Funding sources

We acknowledge the support of the Natural Sciences and Engineering Research Council of Canada (NSERC), [RGPIN-2024-05084].

# References

1. Akagami, R., Dong, C.C.J., Westerberg, B.D., 2005. Localized transcranial electrical motor evoked potentials for monitoring cranial nerves in cranial base surgery. Neurosurgery 57, 78–85; discussion 78-85. https://doi.org/10.1227/01.neu.0000163486.93702.95
2. Baker, M.D., Bostock, H., 1997. Low-threshold, persistent sodium current in rat large dorsal root ganglion neurons in culture. J. Neurophysiol. 77, 1503–1513. https://doi.org/10.1152/jn.1997.77.3.1503
3. Bostock, H., Rothwell, J.C., 1997. Latent addition in motor and sensory fibres of human peripheral nerve. J. Physiol. 498 ( Pt 1), 277–294. https://doi.org/10.1113/jphysiol.1997.sp021857
4. Bostock, H., Lin, C.S.-Y., Howells, J., Trevillion, L., Jankelowitz, S., Burke, D., 2005. After-effects of near-threshold stimulation in single human motor axons: Subthreshold superexcitability. J. Physiol. 564, 931–940. https://doi.org/10.1113/jphysiol.2005.083394
5. Chang, S.D., López, J.R., Steinberg, G.K., 1999. Intraoperative electrical stimulation for identification of cranial nerve nuclei. Muscle Nerve 22, 1538–1543. https://doi.org/10.1002/(sici)1097-4598(199911)22:11<1538::aid-mus8>3.0.co;2-0
6. Crill, W.E., 1996. Persistent sodium current in mammalian central neurons. Annu. Rev. Physiol. 58, 349–362. https://doi.org/10.1146/annurev.ph.58.030196.002025
7. Deletis, V., Fernández-Conejero, I., 2016. Intraoperative monitoring and mapping of the functional integrity of the brainstem. J. Clin. Neurol. 12, 262–273. https://doi.org/10.3988/jcn.2016.12.3.262
8. Dong, C.C.J., Macdonald, D.B., Akagami, R., Westerberg, B., Alkhani, A., Kanaan, I., Hassounah, M., 2005. Intraoperative facial motor evoked potential monitoring with transcranial electrical stimulation during skull base surgery. Clin. Neurophysiol. 116, 588–596. https://doi.org/10.1016/j.clinph.2004.09.013
9. Goto, T., Muraoka, H., Kodama, K., Hara, Y., Yako, T., Hongo, K., 2010. Intraoperative monitoring of motor evoked potential for the facial nerve using a cranial peg-screw electrode and a “threshold-level” stimulation method. Skull Base 20, 429–434. https://doi.org/10.1055/s-0030-1261270
10. Goldin, A.L., 2003. Mechanisms of sodium channel inactivation. Curr. Opin. Neurobiol. 13, 284–290. https://doi.org/10.1016/s0959-4388(03)00065-5

11. Isaacson, B., Kileny, P.R., El-Kashlan, H.K., 2005. Prediction of long-term facial nerve outcomes with intraoperative nerve monitoring. Otol. Neurotol. 26, 270–273. https://doi.org/10.1097/00129492-200503000-00025
12. Irnich W. The terms “chronaxie” and “rheobase” are 100 years old. Pacing Clin Electrophysiol. 2010 Apr;33(4):491–6.
13. Izzo MGA, Rossi Sebastiano D, Catanzaro V, Melillo Y, Togni R, Visani E, et al. Three montages for Transcranial electric stimulation in predicting the early post-surgery outcome of the facial nerve functioning. Clin Neurophysiol. 2024 Nov;167:282–93.
14. Naidoo A, Jones KE. Temporal summation of subthreshold stimuli in human motor axons: supporting data and supplementary materials [dataset]. Figshare; 2025. https://doi.org/10.6084/m9.figshare.29897132.
15. Neuloh, G., Strauss, C., Schramm, J., 2008. Mapping and monitoring for brainstem lesions, in: Handbook of Clinical Neurophysiology. Elsevier Health Sciences, pp. 522–533. https://doi.org/10.1016/S1567-4231(07)08037-9
16. Panizza, M., Nilsson, J., Roth, B.J., Rothwell, J., Hallett, M., 1994. The time constants of motor and sensory peripheral nerve fibers measured with the method of latent addition. Electroencephalogr. Clin. Neurophysiol. 93, 147–154. https://doi.org/10.1016/0168-5597(94)90078-7
17. Sørensen, D.M., Bostock, H., Abrahao, A., Alaamel, A., Alaydin, H.C., Ballegaard, M., Boran, E., Cengiz, B., de Carvalho, M., Dunker, Ø., Fuglsang-Frederiksen, A., Graffe, C.C., Jones, K.E., Kallio, M., Kalra, S., Krarup, C., Krøigård, T., Liguori, R., Lupescu, T., Maitland, S., Matamala, J.M., Moldovan, M., Moreno-Roco, J., Nilsen, K.B., Phung, L., Santos, M.O., Themistocleous, A.C., Uysal, H., Vacchiano, V., Whittaker, R.G., Zinman, L., Tankisi, H., 2023. Estimating motor unit numbers from a CMAP scan: Repeatability study on three muscles at 15 centres. Clin. Neurophysiol. 151, 92–99. https://doi.org/10.1016/j.clinph.2023.04.008
18. Téllez, M.J., Ulkatan, S., Urriza, J., Arranz-Arranz, B., Deletis, V., 2016. Neurophysiological mechanism of possibly confounding peripheral activation of the facial nerve during corticobulbar tract monitoring. Clin. Neurophysiol. 127, 1710–1716. https://doi.org/10.1016/j.clinph.2015.07.042
19. Urriza, J., Arranz-Arranz, B., Ulkatan, S., Téllez, M.J., Deletis, V., 2016. Integrative action of axonal membrane explored by trains of subthreshold stimuli applied to the peripheral nerve. Clin. Neurophysiol. 127, 1707–1709. https://doi.org/10.1016/j.clinph.2015.07.024
20. Urriza, J., 2020. Effects of subthreshold stimuli on the excitability of axonal membrane, in: Neurophysiology in Neurosurgery. Elsevier, pp. 113–118. https://doi.org/10.1016/b978-0-12-815000-9.00008-3
21. Vanderbei, R. J., & Zhang, T. A general reduced gradient algorithm for nonlinear programming. Mathematical Programming. 1991;52(1):77–101.

22. Verst, S.M., Chung, T.M., Sucena, A.C., Maldaun, M.V.C., Aguiar, P.H.P., 2012. Comparison between the C5 or C6-Cz electrode assembly and C3 or C4-Cz assembly for transcranial electric motor activation of muscular response of the contralateral facial nerve. Acta Neurochir. (Wien) 154, 2229–2235. https://doi.org/10.1007/s00701-012-1505-z

## Table legends

**Table 1.** Mean CMAP (± standard deviation) response probabilities per condition, calculated as the grand average across all tests and all participants.

**Table 2.** Subthreshold Susceptibility Index (SSI) values represent the number of stimuli required for a 5% CMAP probability. SSI was determined by curve fitting then solving for the number of stimuli required for a 5% CMAP probability (Eq. 2). No value was calculated for the 80% of threshold with 0.1 ms pulse width condition due to insufficient responses.

## Figure legends

**Fig 1.** Example CMAP recordings from a single participant (APB muscle) showing responses to a single subthreshold pulse and to trains of 2-7 identical subthreshold pulses (0.5 ms pulse width, 85% of threshold intensity, 2 ms ISI). The proportion of trials meeting the CMAP criterion (≥ 100 µV, regardless of latency) was used to calculate response probability. This illustrates how repeated subthreshold pulses can summate to trigger peripheral activation despite the absence of a single-pulse response.

**Fig 2.** Means probability of a CMAP response (± 95% CI) as a function of pulse width for three amplitudes (% of motor threshold). Higher amplitudes and longer pulse widths increased response probability, with a significant amplitude x width interaction. For clarity, data are presented with pulse width on the x-axis; an alternative arrangement using pulse amplitude as the x-axis was considered but deemed redundant, as statistical inferences were consistent across both dimensions (all pairwise comparisons $p \leq .023$). Boxed groups highlight the three amplitudes at each pulse width; the asterisk (*) above each box indicates that all pairwise comparisons within that pulse width were statistically significant.

**Fig 3.** Median probability of CMAP response (%) versus number of stimuli per train for pulse widths of (A) 1.0 ms, (B) 0.5 ms, and (C) 0.1 ms. Curves (fitted to Eq. 1) show that higher amplitudes (% threshold) require fewer stimuli to reach the 5% probability criterion (grey dashed line), used to calculate the Subthreshold Susceptibility Index (SSI). This provides a practical tool for identifying amplitude-width-&-train length combinations that minimize the risk of peripheral activation during IONM.

**Fig 4.** Relationship between mean CMAP response probability and LAh, and index of persistent sodium current. The positive association ($r_{partial}$= .539, p = .047 after controlling for rheobase) indicates that stronger persistent sodium current is linked to greater susceptibility to subthreshold activation. While LAh accounted for ~29% of the variance, substantial unexplained variability suggests additional contributing factors.

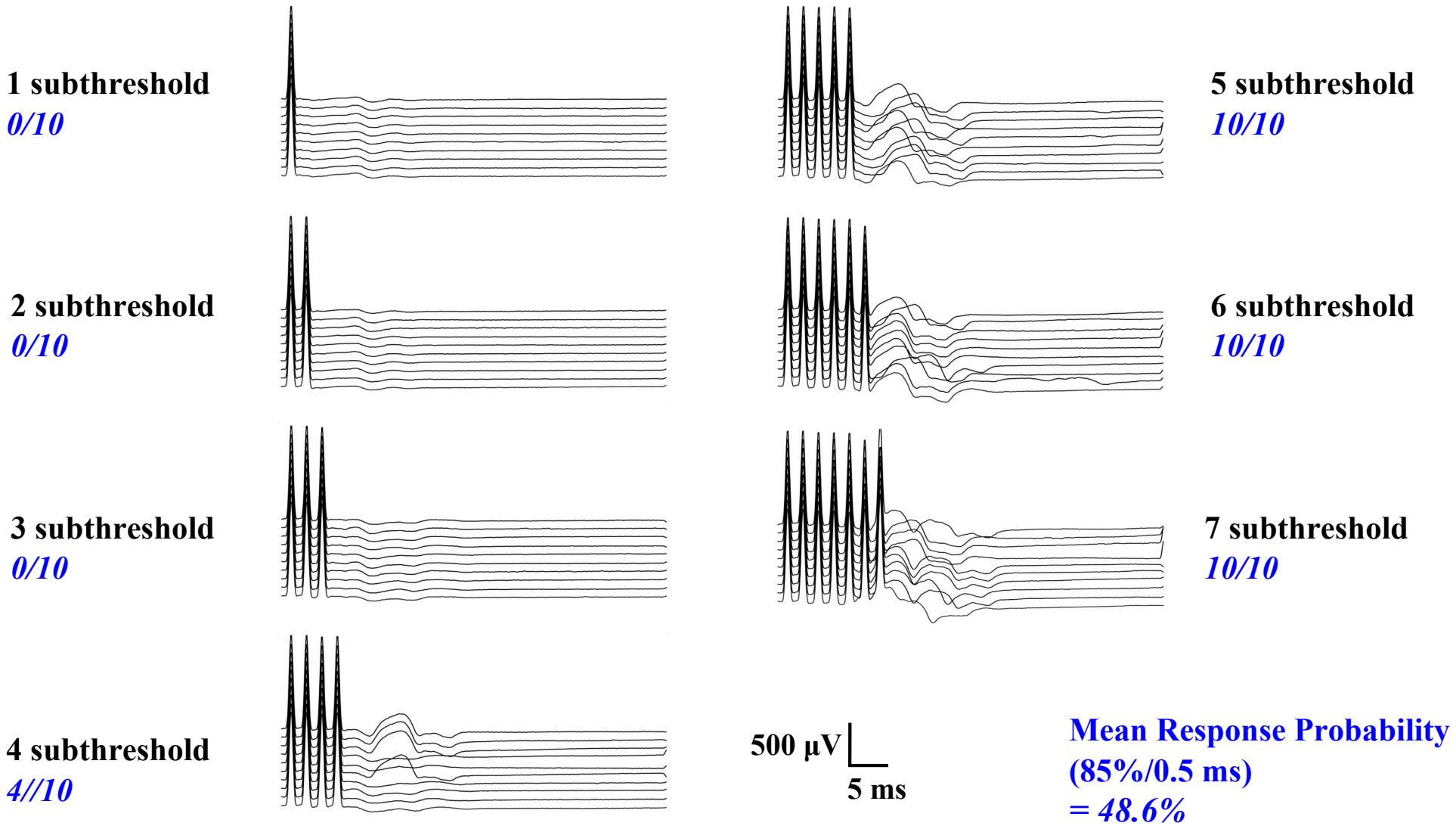
1 subthreshold
0/10
2 subthreshold
0/10
3 subthreshold
0/10
4 subthreshold
4//10
5 subthreshold
10/10
6 subthreshold
10/10
7 subthreshold
10/10
500 µV
5 ms
Mean Response Probability
(85%/0.5 ms)
= 48.6%

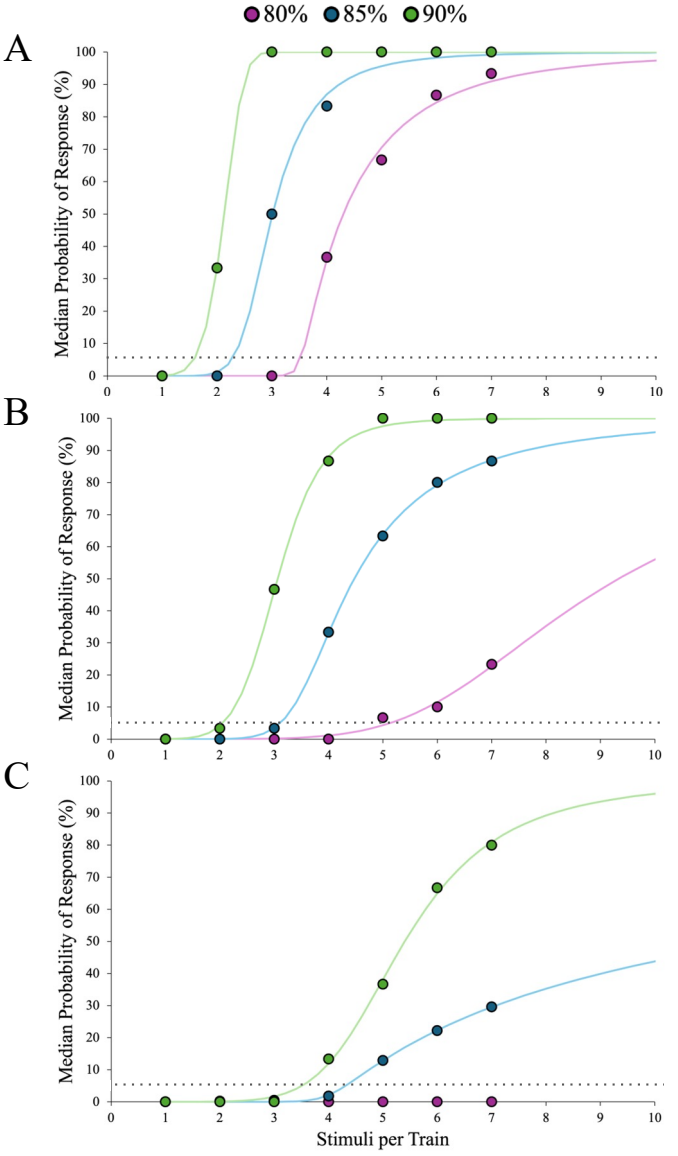
80%
85%
90%
A
B
C
Median Probability of Response (%)
Stimuli per Train
0
1
2
3
4
5
6
7
8
9
10
0
10
20
30
40
50
60
70
80
90
100

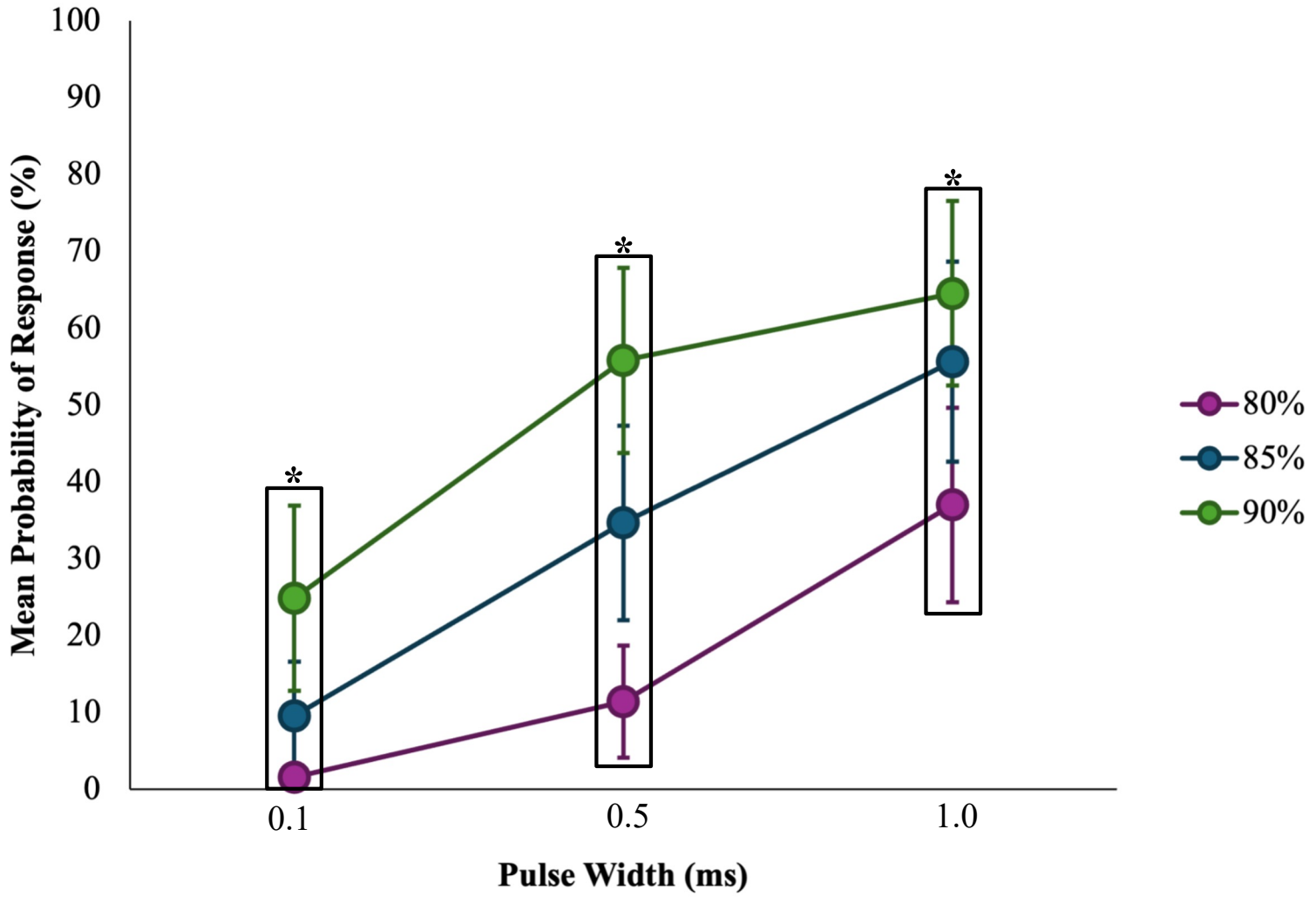
100
90
80
70
60
50
40
30
20
10
0
Mean Probability of Response (%)
*
*
*
0.1
0.5
1.0
Pulse Width (ms)
80%
85%
90%

**Table 1.** Mean CMAP (± standard deviation) response probabilities per condition, calculated as the grand average across all tests and all participants.

| ***Pulse Amplitude (% of threshold)*** | | ***Pulse Width (ms)*** | | |
|---|---|---|---|---|
| | | ***0.1*** | ***0.5*** | ***1.0*** |
| | ***80%*** | 1.6 ± 6.6 | 11.4 ± 23.6 | 37.0 ± 41.8 |
| | ***85%*** | 9.6 ± 22.4 | 34.7 ± 40.2 | 55.7 ± 45.0 |
| | ***90%*** | 24.9 ± 35.8 | 55.8 ± 44.3 | 64.6 ± 44.7 |

**Table 2.** Subthreshold Susceptibility Index (SSI) values represent the number of stimuli required for a 5% CMAP probability. SSI was determined by curve fitting then solving for the number of stimuli required for a 5% CMAP probability (Eq. 2). No value was calculated for the 80% of threshold with 0.1 ms pulse width condition due to insufficient responses.

| ***Pulse Amplitude (% of threshold)*** | | ***Pulse Width (ms)*** | | |
|---|---|---|---|---|
| | | ***0.1*** | ***0.5*** | ***1.0*** |
| | ***80%*** | N/A | 5.1 | 3.5 |
| | ***85%*** | 4.3 | 3.1 | 2.3 |
| | ***90%*** | 3.5 | 2.1 | 1.6 |